ELSEVIER

Applied Surface Science 180 (2001) 65–72

applied surface science

www.elsevier.com/locate/apsusc

Strain in coherent cobalt silicide islands formed by reactive epitaxy

P.A. Bennett[a,*], D.J. Smith[a], I.K. Robinson[b]

[a]*Department of Physics and Astronomy and Science and Engineering of Materials, Arizona State University, Box 871504, Tempe, AZ 85287-1504, USA*
[b]*Department of Physics, University of Illinois, Urbana, IL 61801, USA*

Received 19 February 2001; accepted 14 April 2001

Abstract

We have used surface X-ray diffraction (XRD) to measure strain in coherent islands of cobalt silicide formed by depositing 0–5 ML of cobalt on Si(1 1 1)-7 × 7 at various temperatures. Silicide structure is determined from truncation rod scans, while average island dimensions (width and height) and strain are determined from diffraction lineshapes and verified with TEM. At 800°C, the islands are fully coherent B-type $CoSi_2$, approximately 8 nm thick and >300 nm wide, with atomically flat top and bottom surfaces. At 500°C, the islands are $CoSi_2$, approximately 6 nm thick and 35 nm wide. The lattice parameter is ~50% relaxed, primarily due to strain relief at the island edges. At 300°C and coverage of 2 ML, the islands are ~3 nm high and ~3 nm wide and show long-range position correlation due to registry with the substrate. At higher coverage, they are ~4 nm high and ~40 nm wide and commensurate, but lack long-range correlation. It appears that the silicide formed at 300°C is pseudomorphic Co_2Si-θ for coverage below 2 ML, but is a mixture of $CoSi_2$ and metastable CoSi(CsCl) at higher coverage.
© 2001 Elsevier Science B.V. All rights reserved.

PACS: 68.55; 61.10.-i; 81.15.Tv; 68.35.-p

Keywords: Silicide; Coherent island; Strain; Reactive epitaxy

1. Introduction

Silicide overlayers on silicon have been extensively studied, due largely to their importance in the microelectronics industry where they are used as contacts and interconnects [1]. Extended thin layers with flat interfaces are required for such applications. Several schemes exist for producing such layers: low-temperature co-deposition, heavy-metal interlayers and template layers [2–5]. Silicide island structures, on the other hand, have hardly been studied at all. Such structures are interesting both for practical and fundamental reasons. Nanometer-scale islands have potential application in single-electron devices based on the Coulomb blockade effect. In this context, silicides may be superior to other materials systems, such as nano-crystal silicon, since they can be grown as epitaxial, single-crystal islands with defect-free interfaces and surfaces [6]. Nanometer-scale wires have also been grown, and have potential application as interconnects, again with the advantages of single-crystal structure

* Corresponding author. Tel.: +1-480-965-9623; fax: +1-480-965-7954.
E-mail address: peter.bennett@asu.edu (P.A. Bennett).

0169-4332/01/$ – see front matter © 2001 Elsevier Science B.V. All rights reserved.
PII: S0169-4332(01)00321-X

and perfect interfaces [7]. On a fundamental level, the structure and stability of nanoscale epitaxial islands is intrinsically interesting, and the island formation process provides a context to quantify atomic-level parameters such as surface diffusion and island/step/cluster binding energies, which are entirely unknown for silicide systems [8,9].

Strain plays a dominant role in heteroepitaxial growth, especially for island structures. It causes a variety of phenomena including: misfit dislocation formation, coherent islanding, crystal shape transformations, and ordering in self-organized island arrays [10–15]. Coherent islanding is particularly relevant to the present study. A *coherent island* contains no misfit dislocations. Strain is relieved nonetheless by distortion of the free edges of the island. The degree of relaxation is scale independent, but increases with aspect ratio (height/width) of the island. For example, Johnson and Freund have shown that strain is reduced to zero at the top of a hemispherical island with aspect ratio $h/w = 0.2$ and can even reverse sign for higher aspect ratio [16].

In this paper, we have used surface X-ray diffraction (XRD) to monitor strain evolution during growth of cobalt silicide islands by reactive epitaxy (metal deposition on a heated substrate). Island shapes are determined from in situ diffraction and STM measurements and confirmed by ex situ imaging (TEM, and AFM). Diffraction offers important information that is not available from imaging, namely island strain (from peak positions) and crystal structure (from intensity analysis of truncation rods). Furthermore, the in situ measurement allows for real-time feedback to the growth process. We find a complex interplay of island shape and strain, and even crystal structure during growth at various temperatures and coverages. This complexity is surprising in view of the simple metallurgy of the cobalt–silicon bulk binary system.

2. Background

In practice, silicide films are most often formed by contact reaction (metal deposition followed by annealing). This reaction for cobalt on silicon has been studied by many workers and is documented in review articles [3,5]. $CoSi_2$ forms at $\sim$500°C for metal coverage >10 ML. Its simple lattice type (CaF_2) and close lattice match with silicon (-1.2%) facilitates formation of an atomically perfect interface that can extend over microns. At lower temperatures, metal-rich silicides form. The structure formed at room temperature near the interface has been variously identified as partially ordered $CoSi_2$, [3] pseudomorphic Co_2Si [17] or intermixed and disordered Co_xSi_y [5]. Island structures formed by annealing have been studied using STM [18]. Co-deposition of Co + Si may be used to produce exceptionally well-ordered and flat layers, notably at room temperature [19]. VonKanel et al. have identified an epitaxial strain-stabilized metastable phase CoSi(CsCl) which can be grown by molecular beam epitaxy (MBE) using suitable templates [20,21].

In contrast, cobalt silicide structures formed by reactive epitaxy have barely been studied, presumeably because the resulting island structure is generally undesired. From STM studies, it is known that monolayer-thick islands with nanometer lateral size form at 300°C, [8,22,23] while multi-layer, micron-sized islands form at 800°C [24]. The high temperature equilibrium properties of Co surface phases have been measured using low energy electron microscopy (LEEM) [25,26]. Copel et al. have shown that a hydrogen overlayer increases the density of cobalt silicide islands grown by reactive epitaxy, but structural information was not provided [27]. Using photoemission, Hong et al. have identified CoSi(CsCl) formed by cobalt deposition on top of $CoSi_2$ at 350°C [28].

3. Procedure

Si(1 1 1) samples were prepared from As-doped 0.3 Ω cm, 0.1° miscut wafers, by heating briefly to 1250°C and cooling slowly to produce a clean 7×7 surface. Cobalt metal was deposited by sublimation from a high-purity 0.5 mm diameter wire located 10 cm from the sample. Thickness was monitored in situ using a crystal thickness monitor and calibrated ex situ using RBS, with an overall accuracy of 20%. Temperature above 700°C is determined using an optical pyrometer. Lower temperatures are determined from power versus thermocouple data for a matching sample holder in a separate chamber. All diffraction scans were made at room temperature following

formation of the silicide overlayers. UHV-STM measurements were made on samples prepared in similar fashion in a separate chamber. These samples were also measured ex situ using TEM and AFM. Uncertainties in temperature and coverage calibrations between experiments prevent a detailed comparison of island structure inferred from images versus diffraction.

Diffraction measurements were made on beamline X16A, a dedicated surface. XRD facility at the National Synchrotron Light Source, Brookhaven. Diffraction peaks are indexed on a hexagonal lattice with $(1\,0\,0)_{hex} = 1/3\ \ (4\,\underline{2}\,\underline{2})_{cubic}$ and $(0\,0\,3)_{hex} = (1\,1\,1)_{cubic}$. These reflections comprise the reciprocal lattice units (RLU) for lateral and vertical scans, respectively. Several different epitaxial silicides are possible for the Co/Si(1 1 1) system, as shown in Table 1. Since the silicide islands are mostly commensurate with the substrate 1×1 unit cell, they can only be distinguished by their vertical structure, which we determine using truncation rod scans. Using a wavelength of 1.18 Å. (10.4 keV) and an incidence angle up to 45° allows measurements of Q_{perp} up to 4.5 RLU. Accessible reflections for silicon and various cobalt silicides are shown in Table 1, along with their nominal misfit with the substrate. $CoSi_2$ invariably grows in B-type orientation, whereby the overlayer is rotated 180°. This provides an important practical tool for the diffraction study, since the overlayer Bragg peaks are separated from those of the substrate, allowing great sensitivity to their presence.

Rod scans were compiled in two ways: from integrated rocking scans across the rod at discrete values of L and from continuous scans along the rod. The former yields accurate structure factors with associated corrections for polarization, detector volume, illuminated area, etc [30,31]. The latter is useful for quick inspection and/or high-resolution lineshape measurement in the vertical direction, but does not yield structure factors and is susceptible to misalignment. In some cases, we have combined these two methods by showing $\sqrt{(\text{cnts})}$ for the direct scan, normalized to the rocking curve data at convenient points. Rod scan data are shown as true structure factors unless otherwise stated.

Island dimensions are estimated from the linewidth of silicide Bragg peaks using $\Delta x \sim d_{hkl} \times (G/\Delta Q)$, where d_{hkl} is the plane spacing associated with the unit-defining reflection G and Δx, ΔQ are full-width half-maximum values for average island size and peak width, respectively. Thus, for lateral dimensions we have $d_{1\,0\,0} = 3.32$ Å and for vertical dimensions we have $d_{0\,0\,1} = 9.41$ Å. Typically the scan is made at L values just off the Bragg peak (for example, $L = 4.1$ rather than 4.0) to avoid confusion with extraneous peaks from a small number of large twinned particles that can arise during sample preparation. Diffraction peaks may also be broadened due to strain effects (see below). In principle, one can separate these since linewidth scales with $|Q|$ for strain but is independent of $|Q|$ for finite-size effects [32]. In practice, a complicated lineshape can result, particularly for coherent islands which may have appreciable variation of strain and curvature of atomic layers within the island [33]. Strain (one dimensional) is estimated as $\varepsilon_x = (a - a_0)/a_0 = -(h - h_0)/h_0$, where h is the peak position for strained material, h_0 for unstrained, and $(a,\ a_0)$ are the associated lattice parameters at room temperature. At high temperature, the silicide expands more than the substrate, creating an additional mismatch of about +0.6% at 800°C [5].

Table 1
Nominal Bragg reflections for silicon and various cobalt silicide structures, indexed on the hexagonal lattice[a]

Si	$CoSi_2$	CoSi(CsCl)	Co_2Si-θ
(1 0 4)	(0 1 4)	(0 1 4)	(1 0 ±4)
(1 0 1)	(0 1 1)	(0 1 1)**	(1 0 ±2)*
(0 1 2)**	(1 0 2)*	(1 0 2)	(1 0 0)*
(0 2 4)	(2 0 4)	(2 0 4)	(2 0 ±4)
(0 2 1)	(2 0 1)	(2 0 1)**	(2 0 ±2)*
(2 0 2)**	(0 2 2)*	(0 2 2)	(2 0 0)*
$(\text{Misfit})_{par}$	−1.2%	+0.9%	−1.5%
$(\text{Misfit})_{perp}$	−1.2%	−1.9%	−3.4%

[a] The cubic silicides are shown in B-type orientation whereby $(h\,k\,l)$ of the overlayer maps onto $(-h\ -k\ l)$ of the substrate. Weak peaks (<5% of strongest) are indicated with *, forbidden peaks are indicated with **. Misfit is shown for directions parallel and perpendicular to the surface. Lattice parameters are from Goncalves [20] and Nicolet [29]. Co_2Si-θ is an assumed hexagonal structure isomorphous to bulk-stable Ni_2Si-θ, with lattice parameter scaled from $NiSi_2$ and $CoSi_2$.

4. Results

In Fig. 1 we show images of the silicide islands grown at various temperatures and coverage. This

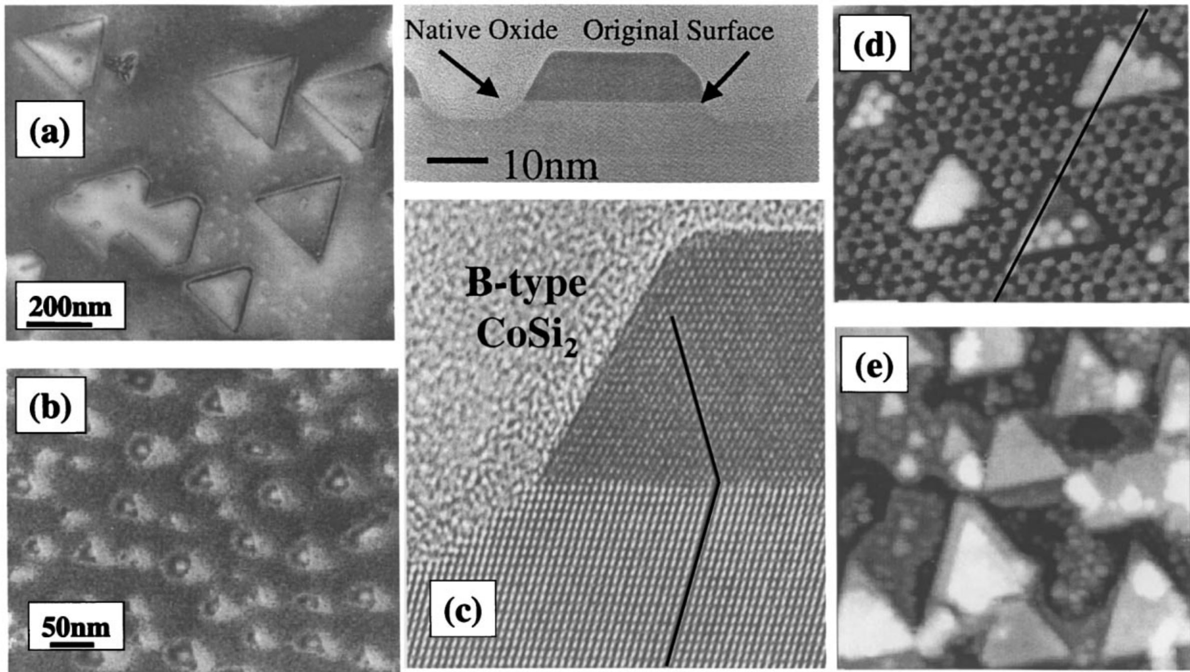

Fig. 1. TEM (panels a–c) and STM (panels d and e) images of islands prepared under conditions similar to the X-ray experiment: (a) 5 ML at 800°C, (b) 5 ML at 500°C, (c) 5 ML at 600°C, (d) 0.25 ML at 320°C scan size $(14\ \text{nm})^2$, (e) 2 ML at 400°C scan size $(25\ \text{nm})^2$.

serves as a useful comparison with the diffraction results, although the errors in temperature and coverage calibration prevent exact correspondence. At 800°C the islands form nearly perfect equilateral triangles ~250 nm wide. This shape follows the three-fold rotational symmetry of the substrate. Most are defect-free, although a small number are highly dislocated. One example is seen in the figure. Pinholes are also visible, but appear to contribute relatively little strain. At 600°C the islands are only ~30 nm wide and have less regular shapes. They are defect-free. The cross-section images show they are B-type $CoSi_2$ with atomically flat top and bottom surfaces and very well defined side facets. In addition, the islands are surrounded by trenches which form during the reaction. This leaves a small pedestal of silicon under each island. At 300°C, the islands are equilateral triangles, nominally two unit cells wide (~6 nm), embedded in the 7×7 reconstruction. At 400°C and somewhat higher coverage, the islands are multi-layered and coalesced.

Diffraction measurements show that islands grown at 800°C are B-type $CoSi_2$ at all coverages. This is seen in the rod scans shown in Fig. 2. The clean surface shows peaks only at $L = +1$ and $+4$ due to the substrate. For 2.6 ML coverage, peaks near $L = -4$ and -1 clearly signify B-type $CoSi_2$. The silicide should also show a weak peak near $L = +2$, but this would only be 10 on this scale, and is not visible in the noise. The direct rod scan at (2 0 4) shows clear interference oscillations which signify atomically flat interfaces on both top and bottom of the silicide crystals as well as a uniform thickness amongst all crystals. From the period of oscillations we derive an island thickness of 7.5 nm. The peak maximum is at $L = 4.09 \pm 0.01$ RLU, corresponding to a vertical strain of $\varepsilon_z = -(4.09 - 4.05)/4.05 = -1.0 \pm 0.2\%$.

Transverse radial scans through the silicide peaks are shown in Fig. 3 for 2.6 ML coverage. The lineshape is invariant with coverage. We compare peaks at two values of $|Q|$ to separate strain from size effects. The peak maxima are shifted in proportion to $|Q|$, reflecting the average strain in the islands. The maximum of the (0 2 4.1) peak occurs at $k_0 = 2.003 \pm 0.001$ corresponding to a strain of

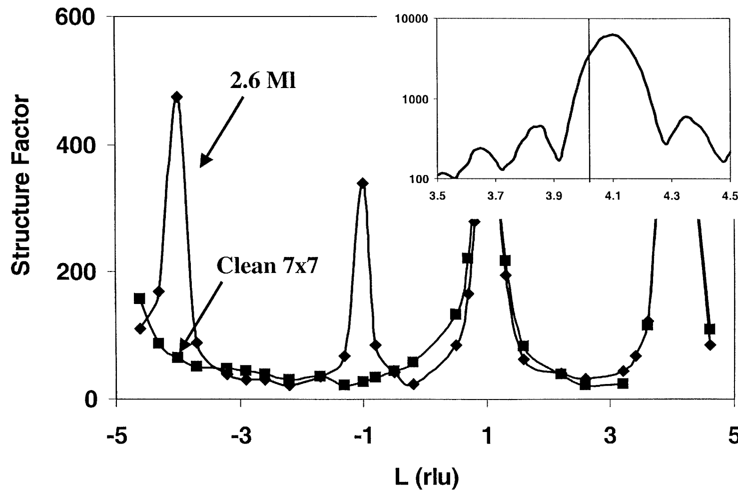

Fig. 2. (1, 0) rod scans for clean 7 × 7 and 2.6 ML at 800°C. The inset is a direct rod scan along the (2, 0) rod, which shows interference oscillations due to sharp top and bottom surfaces of the silicide. The vertical line marks the unstrained peak position at $L = 4.05$ RLU.

$\varepsilon_x = -(2.003 - 2.02)/2.02 = +0.9 \pm 0.05\%$. The peak shift is half this amount for the (1 0 4.1) peak, meaning that the strain is isotropic, as expected. The lateral and vertical strain values are consistent with elasticity theory, which predicts $\varepsilon_z = -2\nu/(1-\nu)\varepsilon_x \sim -\varepsilon_x$ for biaxial strain ($\varepsilon_x = \varepsilon_y$), using a value of $\nu \sim 1/3$ for Poisson's ratio. The measured average lateral strain is somewhat smaller than that of a fully strained uniform overlayer (1.2%). Since the island aspect ratio is only 7.5/200 = 0.04, this strain relaxation is not likely due to the free island edges. We believe it is primarily due to the silicon pedestal underlying the silicide island. Recall that the diffraction "sees" only the silicide because of the B-type epitaxy, and the free edges of the silicon pedestal should considerably relieve stress. Lastly, we note that the broad tail in the lineshape is essentially independent of $|Q|$, implying that it arises primarily

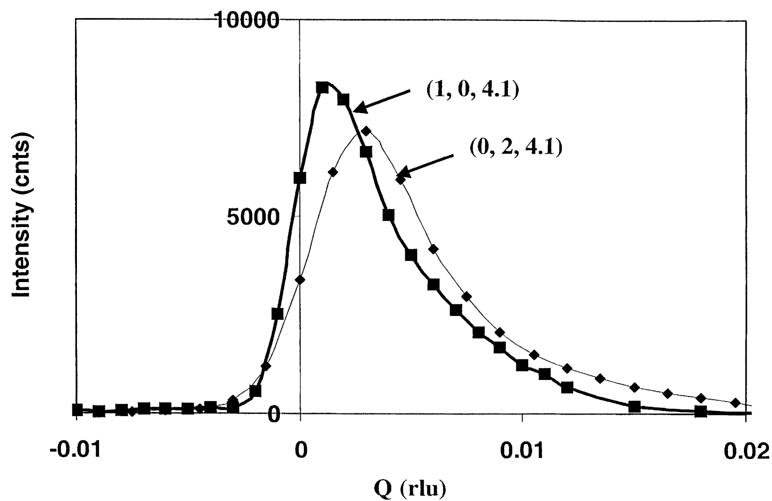

Fig. 3. Transverse radial lineshape at $Q = (0\,1\,4.1)$ and $(2\,0\,4.1)$ for 2.6 ML at 800°C. The RLU for lateral measurements is defined by the (1 0 0) reflection. The Q-axis has been shifted (not scaled!) such that zero marks the commensurate position for each peak.

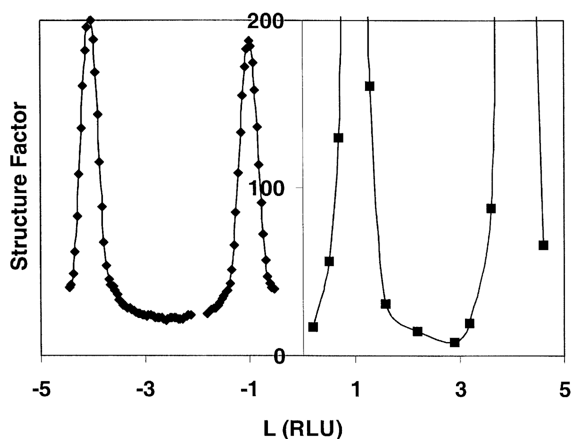

Fig. 4. (1, 0) rod scan for 2.1 ML at 500°C. Values for $L > 0$ are true structure factors derived from rocking curves. Values for $L < 0$ are derived from direct rod scans (see text). The presence of peaks at $L = -4$, -1 not $+2$ indicates pure B-type $CoSi_2$.

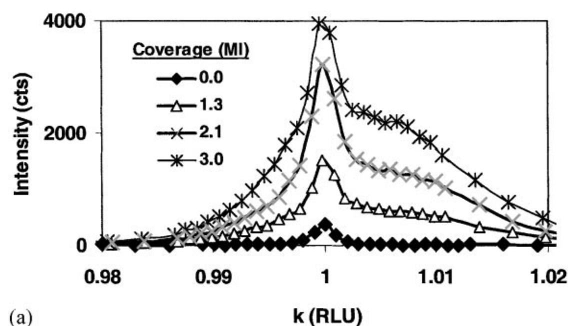

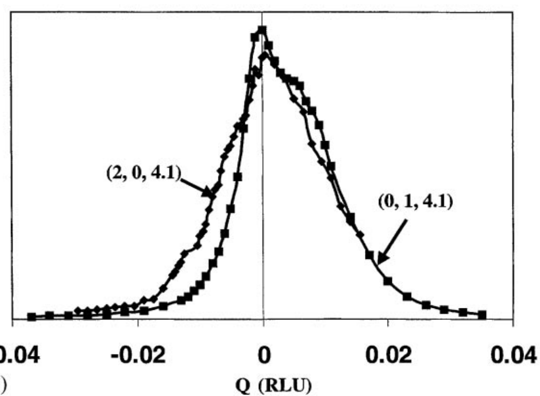

Fig. 5. (a) Transverse radial lineshape at $Q = (0\,1\,4.1)$ for growth at 500°C. (b) Transverse radial lineshapes at $Q = (0\,1\,4.1)$ and $(2\,0\,4.1)$ for 2.1 ML grown at 500°C. The vertical axis is linear. The peaks have been shifted laterally to align the maxima.

from finite-size effects. This is consistent with scattering from a small number of highly dislocated islands, as seen in the TEM images.

Islands grown at 500°C again are B-type $CoSi_2$ at all coverages, as seen in the rod-scans in Fig. 4. In this case, there are no interference oscillations, signifying that the island thickness is variable, either within a single island and/or amongst the distribution of islands. From the width of the rod scan near $L = -4$, we find an island height of ~7 nm. The peak maximum is at $L = 4.06 \pm 0.005$ RLU, corresponding to a vertical strain of $\varepsilon_x = -(4.06 - 4.05)/4.05 = -0.2 \pm 0.1\%$ or essentially zero within the error.

Transverse radial scans through the (0 1 4.1) silicide peak for growth at 500°C are shown in Fig. 5a. The lineshape is essentially invariant with coverage. It has a resolution-limited component at the commensurate position and a broad shoulder centered at $k_0 = 1.0044 \pm 0.001$ RLU. This is an intrinsic lineshape rather than a composite from different islands since the shoulder and sharp peak have the same structure along L and because the lineshape is independent of coverage. In Fig. 5b, we compare radial lineshapes for different $|Q|$, and see that the broad component is independent of $|Q|$, implying it originates from finite size effects. The corresponding island lateral size is 40 nm. The shift of the broad shoulder corresponds to a lateral strain $\varepsilon_x = -(1.0044 - 1.01)/1.01 = +0.6 \pm 0.1\%$. This is only 50% of the value of fully strained silicide. We believe it is primarily due to strain relaxation at the free island edges. The island height/width ratio is ~7/40 = 0.2, hence such relaxation may be appreciable. For these islands, the lateral and vertical strains do not agree with simple elastic theory for an extended solid. This is likely due to the variation of strain within the island.

Islands grown at 300°C show a pronounced variation with coverage. At 3.9 ML, the rod-scans (Fig. 6) indicate the presence of both $CoSi_2$ with peaks at $L = -4$, -1 not $+2$ and CoSi(CsCl) with peaks at $L = -4$, $+2$ not -1. Both have B-type orientation. At 2.1 ML, the silicide shows only the peak at $L = -4$. This latter structure is consistent with Co_2Si-θ (see Table 1). It is not surprising that $CoSi_2$ and CoSi(CsCl) are intermixed, since they share the same lattice structure. That is, CoSi(CsCl) can be formed by putting Co at the interstices of the $CoSi_2$ structure. It is not clear why Co_2Si-θ should form at low coverage,

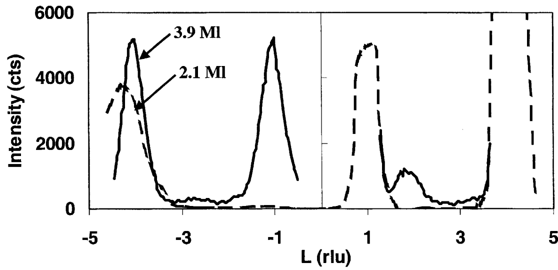

Fig. 6. (1, 0) rod scans for growth at 300°C. At 3.9 ML the structure is a mix of $CoSi_2$ and CoSi(CsCl), both with B-type orientation. At 2.1 ML, it is Co_2Si-θ (see text).

followed by $CoSi_2$, since one might expect the stoichiometry to evolve in the reverse order (silicon rich at first). However, these are ultrathin overlayers, and surface/interface energies are expected to dominate metallurgical parameters as described for this system by von Kaenel et al. [21].

Transverse radial scans through the silicide peak at $Q = (0\,1\,4.1)$ are shown in Fig. 7. Below 3 ML, the peak has two components: one is resolution-limited the other is broad but both are centered at the commensurate position. With increasing coverage, the narrow peak disappears, and the broad component suddenly becomes much larger, implying a conversion from one phase into another. The two-component lineshape is consistent with small epitaxial islands whose centers are long-range correlated due to registry with the substrate. The disappearance of the narrow feature at higher coverage implies a disruption of the ordering, perhaps due to strain associated with island coalescence. The $|Q|$ dependence of the radial

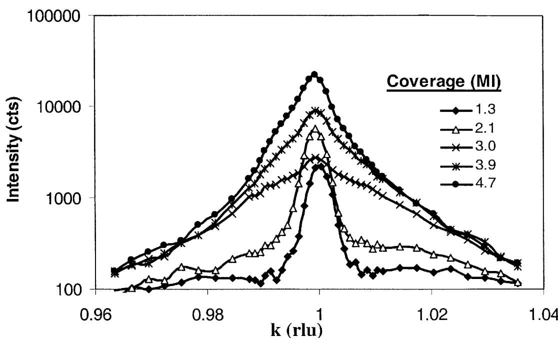

Fig. 7. Transverse radial lineshape at $Q = (0\,1\,4.1)$ for growth at 300°C. Note the log scale for intensity.

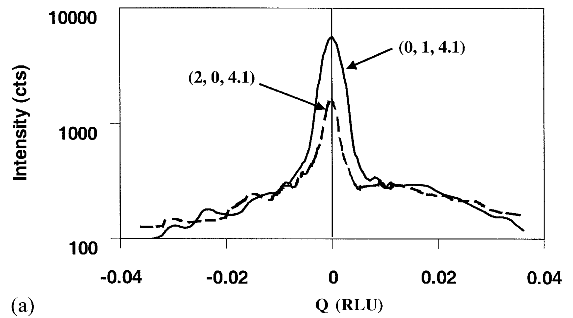

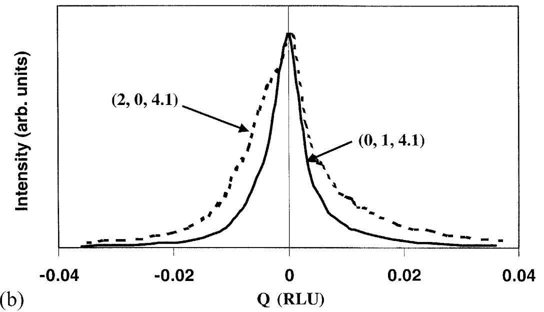

Fig. 8. (a) Transverse radial lineshapes at $Q = (0\,1\,4.1)$ and $(2\,0\,4.1)$ for 2.1 ML at 300°C. Note the log scale for intensity. The peaks have been shifted laterally to align the maxima. (b) Same as above, but coverage is 4.7 ML and the intensity scale is linear.

lineshape is shown in Fig. 8. At low coverage, the broad component is independent of $|Q|$, indicative of finite size broadening with island size ~3 nm. Strain cannot be determined accurately for such a broad peak. At higher coverage, the broad component narrows considerably and is clearly shifted from the commensurate position. The compressive strain is consistent with (partial) formation of CoSi(CsCl) which has a positive misfit (see Table 1). The peak width scales with $|Q|$, indicative of strain. The structure inferred from diffraction is consistent with STM images as shown in Fig. 1. At low coverage, the islands are ~6 nm wide, epitaxial, commensurate and embedded in the 7×7 reconstruction. At higher coverage, they are multi-layered and coalesced.

5. Summary and conclusion

Using surface XRD, we have documented the variation of crystal structure and island dimensions

for cobalt silicide islands formed on Si(1 1 1) by reactive epitaxy for 0–5 ML at 300–800°C. At 800°C, the islands are purely B-type $CoSi_2$, atomically flat, nearly 1 mm wide and very thin. Lateral strain matches the misfit, and vertical strain follows simple elasticity theory for a biaxial-strained uniform overlayer. At 500°C, the islands are again purely B-type $CoSi_2$, ~35 nm wide and 6 nm thick. Lateral strain is only 50% of the misfit, primarily due to strain relief at the free island edges. Strain in the silicide is further reduced by self-formed pedestals of silicon that underlie the silicide islands. At 300°C, the island growth is much more complex. The crystal structure is a mixture of $CoSi_2$, metastable CoSi(CsCl) and pseudomorphic Co_2Si-θ. The proportion varies with coverage in the 0–5 ML range and is presumeably determined by thickness-dependent stoichiometry plus surface and interface energies. Island dimensions vary with coverage, being: height ~3 nm and width approximately 3–40 nm. At submonolayer coverage, the islands are only 3 nm wide due to interaction with the 7×7 reconstruction which "quantizes" the island dimensions and orders their lateral position. At higher coverage, the islands are much wider, most likely due to coalescence. Strain becomes compressive, due to island impingement and/or admixture of CoSi(CsCl) which has a positive misfit with silicon.

The rich variation with growth temperature of crystal structure and island size and shape is remarkable, particularly in view of the relatively simple behavior of uniform cobalt silicide overlayers. This illustrates the important role of surface and interface energies in ultrathin films and strain relief in coherent nanoscale island structures.

Acknowledgements

This work was carried out (in part) at the National Synchrotron Light Source, Brookhaven National Laboratory, which is supported by the U.S. Department of Energy, Division of Materials Sciences and Division of Chemical Sciences. The work was supported also by the National Science Foundation under grants DMR99-81779 (PAB), DMR96-32635 (ASU MRSEC) and DMR98-76610 (IKR).

References

[1] A.H. Reader, A.H. van Ommen, P.J.W. Weijs, R.A.M. Wolters, D.J. Oostra, Rep. Prog. Phys. 56 (1993) 1397–1467.
[2] R.T. Tung, Appl. Surf. Sci. 117/118 (1997) 268–274.
[3] R.T. Tung, Mater. Chem. Phys. 32 (1992) 107–133.
[4] R.T. Tung, F. Schrey, Appl. Phys. Lett. 55 (1989) 256–258.
[5] H. von Kaenel, Mater. Sci. Rep. 8 (1992) 193–269.
[6] J.R. Tucker, C. Wang, T.C. Shen, Nanotechnology 7 (1996) 275–287.
[7] Y. Chen, D.A.A. Ohlberg, G. Medeiros-Riberiro, Y.A. Chang, R.S. Williams, Appl. Phys. Lett. 76 (2000) 4004–4006.
[8] P.A. Bennett, H.V. Kaenel, J. Phys. D Appl. Phys. 32 (1999) R71–R87.
[9] J.A. Venables, G.D.T. Spiller, M. Hanbucken, Rep. Prog. Phys. 47 (1984) 399.
[10] A.J. Schell-Sorokin, R.M. Tromp, Phys. Rev. Lett. 64 (1990) 1039–1042.
[11] J. Tersoff, R.M. Tromp, Phys. Rev. Lett. 70 (1993) 2782–2785.
[12] J. Tersoff, A.W. Denier van der Gon, R.M. Tromp, Phys. Rev. Lett. 70 (1993) 1143–1146.
[13] F.M. Ross, J. Tersoff, R.M. Tromp, Phys. Rev. Lett. 80 (1998) 984–987.
[14] D.J. Eaglesham, R. Hull, Mater. Sci. Eng. B 30 (1995) 2–3.
[15] J.A. Floro, et al., Phys. Rev. Lett. 80 (1998) 4717–4720.
[16] H.T. Johnson, L.B. Freund, J. Appl. Phys. 81 (1997) 6081–6090.
[17] J.M. Gibson, J.L. Batstone, R.T. Tung, Appl. Phys. Lett. 51 (1987) 45–47.
[18] B. Ilge, G. Palasantzas, J. De Nijs, L.J. Geerligs, Surf. Sci. 414 (1998) 1–2.
[19] R.T. Tung, F. Schrey, S.M. Yalisove, Appl. Phys. Lett. 55 (1989) 2005–2007.
[20] S. Goncalves-Conto, et al., Phys. Rev. B55 (1997) 7213–7221.
[21] H. von Kaenel, et al., Phys. Rev. Lett. 74 (1995) 1163–1166.
[22] P.A. Bennett, S.A. Parikh, M.Y. Lee, D.G. Cahill, Surf. Sci. 312 (1994) 377–386.
[23] P.A. Bennett, S.A. Parikh, D.G. Cahill, J. Vac. Sci. Technol. A11 (1993) 1680–1685.
[24] F.M. Ross, P.A. Bennett, R.M. Tromp, J. Tersoff, M. Reuter, Micron 30 (1999) 21–32.
[25] R.J. Phaneuf, Y. Hong, S. Horch, P.A. Bennett, Phys. Rev. Lett. 78 (1997) 4605–4608.
[26] R.J. Phaneuf, et al., Surf. Sci. 431 (1999) 232–241.
[27] M. Copel, R.M. Tromp, Appl. Phys. Lett. 65 (1994) 3102–3104.
[28] S. Hong, P. Wetzel, G. Gewinner, C. Pirri, J. Vac. Sci. Technol. A 14 (1996) 3236–3244.
[29] M.A. Nicolet, S.S. Lau, Formation and characterization of transition-metal silicides, in: N.G. Einspruch, G.B. Larrabee (Eds.), VLSI Microstructure Science, Academic Press, New York, 1983, pp. 330–465.
[30] I.K. Robinson, Rep. Prog. Phys. 55 (1992) 599–651.
[31] I.K. Robinson, Phys. Rev. B 33 (1986) 3830–3835.
[32] B.E. Warren, X-ray Diffraction, Addison-Wesley, Reading, MA, 1969.
[33] T. Wiebach, et al., Phys. Rev. B61 (2000) 5571–5578.